Desalination and Water Treatment
www.deswater.com
doi: 10.5004/dwt.2020.25524

جمعية علوم وتقنية المياه
Water Sciences and Technology Association

Modeling of temperature governed saturation states and metal speciation in the marine waters of Kuwait Bay – concern to the desalination process

Chidambaram S, Harish Bhandary, Asim Al-Khalid

Water Research Center, Kuwait Institute for Scientific Research, Safat, Kuwait

ABSTRACT

There is a change in temperature in the marine waters of Kuwait bay with respect to season and daily temperature. This variation in temperature affects the saturation and the speciation states of ions in the marine waters, which serve as the main source of desalination. The change in the saturation states of compounds constituted by major ions and the speciated metal ligands cause a differential impact on the RO membranes. This variation in temperature was considered and modeled using the average bay water composition to determine the saturation state of minerals concerning temperature. This composition was studied for variation from 10°C to 50°C using geochemical model PHREEQC. The metals such as B, Li, Sr, Ba, Fe, Mn, Be, Co, Cr, Ni, Se, Al, Mo and As were analysed in these water and the predominant species of these metals along with their variation with respect to temperatures considered were studied. The saturation states of calcium carbonates and calcium sulfates were considered as they form the significant major ions of marine waters. The order of state of saturation index (SI) is observed to be as, $SI_{Dol} > SI_{Cal} > SI_{Ara} > SI_{Gyp} > SI_{Anhy}$. There is a sharp decrease of pH with respect to increase in temperature was observed. The observation indicates the fact that beyond 25°C there is a decrease in the SI_{Cal}, SI_{Ara}, SI_{Dol} and there is an increase in the SI Anhy. Hence, it is inferred that the SI of carbonate minerals beyond 25°C is slightly reduced and that of sulfate minerals with respect to Ca are increased. This is mainly due to the preferential attraction of Ca to SO_4^{2-} than to CO_3^{2-} above this temperature, which is a reflex of common ions effect. Further it should be noted that pH of the water decreases with temperature and this indirectly affects the HCO_3 concentration in water. So, it is inferred that the carbonate salts are more prominent during winter and the sulfates during summer, and the pre-treatment should also be planned considering the saturation states of water with respect to season.

Keywords: pH; Saturation; Carbonate; Sulfate; Season

1. Introduction

The process of desalination has been studied by various authors for the salt deposits in the membranes (Rawajfeh et al. 2012). The formation of salts is dependent on several factors such as feed water composition (Hamdona et al. 1993), temperature (Amjad and Hooley 1986), pH (Klepetsanis and Koutsoukos 1989), operating pressure (Lee and Lee, 2000), flow velocity (Lee and Lee 2005), permeation rate (Wang et al. 2002). The studies have also proved high salt levels near the membrane, surface, where the particles are expected to be deposited. This has resulted mainly due to the concentration polarization which plays an essential role in the formation of scales in high pressure membrane system (Lee et al. 1999; Chong and Sheikholeslami 2001; Dydo et al. 2003). The rejects are observed to be accumulated in the surface of membrane (Hoef et al. 2008). It was very significant to note that the saturation state is higher at the surface of the membrane surface though the solution may be under saturated or near saturated (Antony et al. 2011). Apart from the surface precipitation, the deposition of salts along the membrane pores was also subsequently studied by various researchers (Oh et al. 2009; Darton et al. 2001). The studies Sheokholeslami and Ng (2001), and Sheikholeslami

Presented at the 13th Gulf Water Conference – Water in the GCC: Challenges and Innovative Solutions. 12–14 March 2019, Kuwait

(2003a, 2003b) inferred that involvement of minor quantities of a different precipitating salt will affect the salt structure, its precipitation and thermodynamic properties. As the salts may act as a seed or absorbent or may dissolve or may contribute to the growth of salts (Nancollas and Zieba 1995; Klepetsanis 1995; Sheikholeslami 2003). Hence the study of co-precipitation of several salts simultaneously forms a feed solution which is complex. In this scenario, the feed water composition for the RO process (Kuwait Bay water) was studied by varying temperature to understand the co-precipitation behavior of predominant salts. An attempt was also made to understand the saturation state of oxides and hydroxide minerals in the membrane, thereby inferring the expectable salts to be precipitated in the membrane with respect to season.

2. Methodology

The average composition of 20 Kuwait Bay water samples was considered for the study (Table 1). Disequilibrium indices Log (IAP/KT) was calculated by PHREEQC (Parkhust and Appelo, 1999) for those minerals and other solids stored in the model data book for which the dissolved constituents are reported in the groundwater analysis.

Solubility equilibrium hypothesis was tested by computing ion activity product (IAP) from the activities of uncomplexed ions based on the stoichiometries of minerals and other solids in the WATEQ4F data base. The activity product is then compared with the solubility product (KT) for the same solid phases to the assumption that certain dissolved constituents in groundwater are in equilibrium with particular minerals and amorphous solids. Disequilibrium indices log (IAP/KT) were calculated to determine, if the water is in thermodynamic equilibrium log (IAP/KT = 0), oversaturated log (IAP/KT > 0) or undersaturated log (IAP/KT < 0) with respect to certain solid phases (Trusdell and Jones 1973). The variation of temperature to determine the influence of season was carried out in PHREEQC modeling by considering a variation of temperature from 10°C to 50°C. The model was considered for saturation index of the minerals as presented in Table 2.

3. Results and discussion

Scaling in industrial processes is plagued by the subsequent factors: (i) flow field, that is, speed of flow and solid/liquid interface conditions; (ii) substrate properties, that is, materials properties and surface conditions; (iii) bulk variables and composition, pH scale buffering capability, chloride and sulfate concentrations, and concentration of dissolved oxygen and (iv) thermal, that is, bulk temperature, surface temperature and heat flux. Surface crystallization happens because of the lateral growth of the size deposit on the membrane surface, leading to flux decline and surface blockage. Bulk crystallization arises once crystal particles square measure shaped within the bulk part through homogeneous crystallization and will deposit on membrane surfaces as sediments/particles, to create a cake layer that ends up influx decline. Additionally, concentrated scale forming conditions ends up in scale growth and agglomeration. This can be because of the random collision of ions with particles and secondary crystallization happens (Chidambaram et al. 2011) on the surface of those foreign bodies gift within the bulk part (Pervov 1991, Okazaki and Kimura 1984), coincidental bulk and surface crystallization can also occur for prime recovery in operation conditions. There are several elements/parameters considered in the study to understand the coprecipitation nature of the salts by calculating the saturation index calculations. Though there are several mineral saturation states and their saturation indexes can be classified into carbonates, sulfate, hydroxides, oxides, aluminosilicates, metal silicates, silicates, fluoride and phosphates. The present study will be concentrating more about, the most predominant form of saturation index carbonates and sulfates.

The chief minerals saturated in carbonates are in the following order, dolomite > huntite > magnesite > calcite > aragonite (Fig. 1). Other carbonate minerals are undersaturated indicating the fact that the saturated minerals tend to form scales or salt deposits in the membrane. The temperature variation studies indicate that saturated carbonates do not show much variation with increase in temperature of the feed solution except for that of huntitie and magnesite saturation, which increases with temperature. The morphological changes of $CaCO_3$ by crystallization and transformation were projected to be controlled by the particle activity product (IAP) (Pena et al. 2010, Ogino et al. 1987). Sawada (1997) deduced a time sequence through the amendment within the exponent of IAP at 25°C, numerous studies (Tzotzi et al. 2007, Chakraborthy et al. 1994, Greenlee et al. 2010, Rodriguez-Blanco et al. 2011) recommend that temperature- and pH-dependent scale are vital factors dominant in the formation of the ultimate crystalline section. Amorphous calcium carbonate can rework to calcite at low temperatures (<30°C) and to aragonite at higher temperatures (≥40°C; Rodriguez-Blanco et al. 2011). Though calcite presents the best physical stability beneath close conditions, the thermodynamically less stable mineral state of aragonite could also be stable beneath such temperature conditions or within the presence of alternative ions or inhibitors. Mg ions in

Table 1
All values in mg/L except for temperature in °C

Al	HCO_3	As	B	Ba	Br	Ca	Cl	Cu	F	Fe	K	Li	Mg	Mn	NO_3	Na	Ni	P	pH	SO_4	Si	Sr	Temp
0.070319	137.75	0.002999	4.87375	0.011735	85.48188	588.1163	26449.43	0.009735	3.273688	0.004207	524.79	0.286313	1711.325	0.000274	0.66121	14554.5	0.00056	0.052593	8.123	3694.4	0.288184	7.2475	24

Table 2
Saturation indexes considered for study with their chemical formulae

Carbonates and its composition		Oxides and its composition	
Aragonite	$CaCO_3$	Birnessite	MnO_2
Artinite	$MgCO_3{\cdot}Mg(OH)_2{\cdot}3H_{2O}$	Bixbyite	Mn_2O_3
Calcite	$CaCO_3$	Bunsenite	NiO
	$CuCO_3$	Hausmannite	Mn_3O_4
Dolomite	$Ca\ Mg(CO_3)_2$	Halmatite	Fe_2O_3
Huntite	$Ca\ Mg_3(CO_3)_4$	Magnetite	Fe_3O_4
Magnesite	$MgCO_3$	Nsutite	MnO_2
Malachite	$Cu_2(OH)_2(CO_3)_2$	Pyrolusite	MnO_2
Natron	$Na_2CO_3{\cdot}10H_2O$	**Aluminosilicates and silicates and its composition**	
Nesquehonite	$Mg\ CO_3{\cdot}10H_2O$	Adularia	$KAl\ Si_3O_8$
	$NiCO_3$	Albite	$NaAl\ Si_3O_8$
Rhodochrosite	$MnCO_3$	Analcime	$NaAl\ Si_2O_6{\cdot}H_2O$
Siderite	$FeCO_3$	Chlorite	$Mg_5Al_2\ Si_3O_{10}{\cdot}(OH)_8$
Strontianite	$SrCO_3$	Chrysolite	$Mg_3\ Si_2O_5(OH)_4$
Witherite	$BaCO_3$	Clinoenstatite	$MgSiO_3$
Hydromagnesite	$Mg_5(CO_3)_4(OH)_2{\cdot}4H_2O$	Halloysite	$Al_2Si_2\ O_5(OH)_4$
Sulfates and its composition		Illite	$K\ Mg\ Al\ Si\ O_{10}(OH)_2$
Anhydrite	$CaSO_4$	Kaolinite	$Al_2Si_2\ O_5(OH)_4$
Antlerite	$Cu\ _3(OH)_4SO_4$	K. Mica	$KAl_3Si_3\ O_{10}(OH)_2$
	$Ba_3(ASO_4)$	Laumontite	$Ca\ Al_2Si_4\ O_{12}{\cdot}4H_2O$
Barite	$BaSO_4$	Leonhardite	$Ca_2\ Al_4Si_8\ O_{24}{\cdot}7H_2O$
Basaluminite	$Al_4(OH)_{10}SO_4$	Montmorillonite	
Celestite	$SrSO_4$	Phyllipsite	$Na_{0.5}K_{\ 0.3}Al\ Si_3\ O_8{\cdot}H_2O$
Chalcanthite	$CuSO_4.5H_2O$	Phlogopite	$K\ Mg_3\ AlSi_3\ O_{10}(OH)_2$
Epsomite	$MgSO_4.7H_2O$	Prehnite	$Ca_2Al\ _2Si_3\ O_{10}(OH)_2$
Gypsum	$CaSO_4.2H_2O$	Pyrophyllite	$Al_2Si_4\ O_{10}(OH)_2$
Turbanite	$Al\ OH\ SO_4$	Chalcedony	SiO_2
Mirabilite	$Na_2\ SO_4.10H_2O$	Quartz	SiO_2
	$MnSO_4$	Sepiolite	$Mg_2\ Si_3O_{7.5}\ OH.\ 3H$
Thenardite	$Na_2\ SO_4$	Talc	$Mg_3\ Si_4O_{10}(OH)_2$
Alunite	$KAl_3(SO_4)_2(OH)_6$	Tremolite	$Ca_2\ Mg_5\ Si_8\ O_{22}(OH)_2$
Jarosite	$K\ -\ KFe_3(SO_4)_2(OH)_6$	Cristobalite	SiO_2
	$Na\ -\ NaFe_3(SO_4)_2(OH)_6$		
Hydroxides and its composition		Diopside	$CaMgSi_2O_6$
$Al(OH)_3$		**Phosphates and fluorides and its composition**	
Boehmite	AlOOH	FCO_3 apatite	$Ca_{10}\ Na$
			$Mg(PO_4)_5(CO_3)\ F$
$Cu(OH)_2$		Fluorapatite	$Ca_5(PO_4)_3\ F$
Brucite	$Mg(OH)_2$	Fluorite	CaF_2
Diaspore	AlOOH	Hydroxyapatite	$Ca_5(PO_4)_3\ OH$
	$Fe(OH)_3$		$Mn\ HPO_4$
Gibbsite	$Al(OH)_3$		$Sr\ F_2$
Goethite	FeOOH	Strengite	$Fe\ PO_4{\cdot}2H_2O$
Manganite	MnOOH		
	$Ni(OH)_2$	Halite	NaCl
Portlandite	$Ca(OH)_2$		
Pyrochrosite	$Mn(OH)_2$		

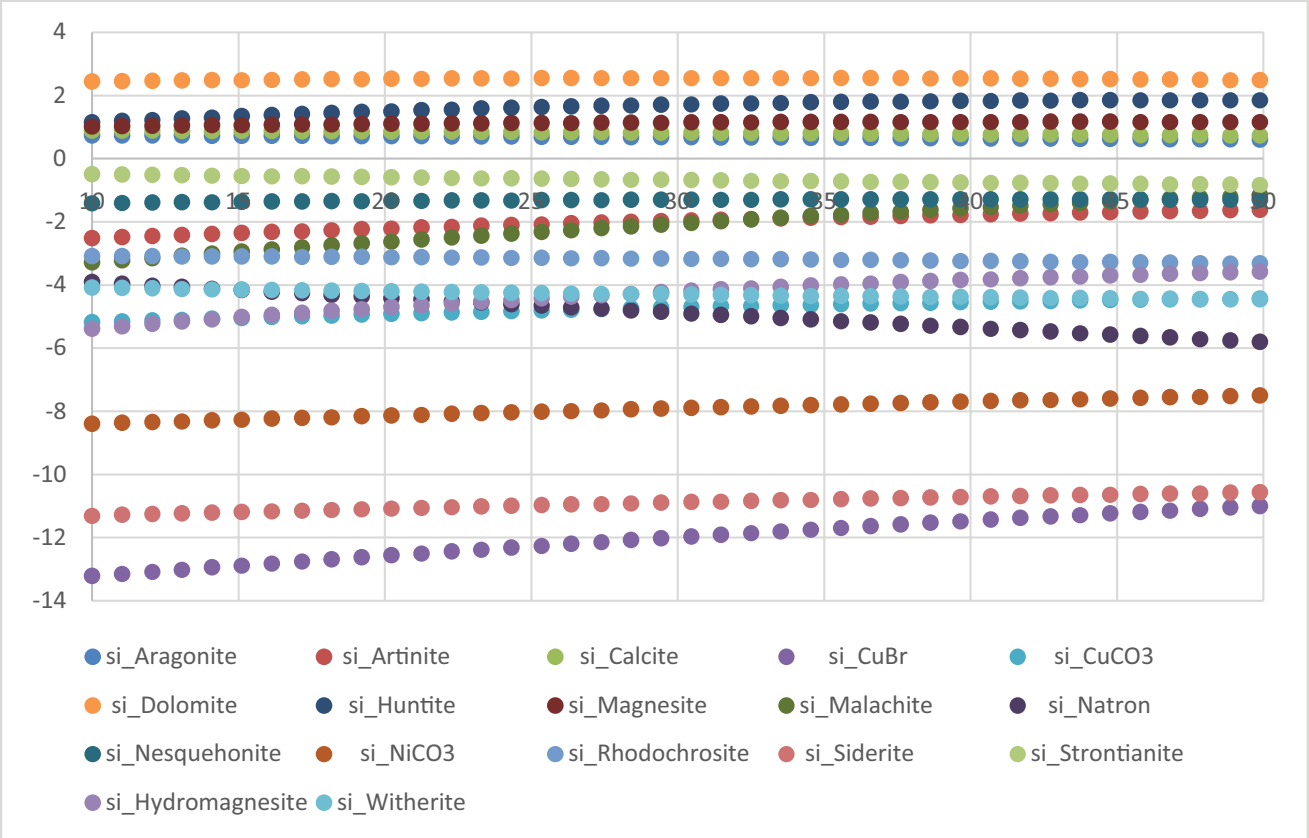

Fig. 1. Variation of the saturation states of carbonate minerals with respect to temperature in °C.

solutions saturated with $CaCO_3$ hinder the formation of vaterite and should favor the precipitation of aragonite mineral (Reddy and Nancollas 1976). Mg in water beside atomic number exerts a profound restrictive result on $CaCO_3$ precipitation evident from literature (Astilleros et al. 2010, Chen et al. 2006, Mucci and Morse 1983).

The variation of temperature with respect to pH and ionic strength of the solution shows that the there is an inverse relationship of these parameters. This variation in pH thus governs the precipitation of carbonate minerals. However, there is a direct relation to temperature and pCO_2 values in the solution (Fig. 2). The earlier studies infer that the carbonate precipitations are chiefly governed by pH and pCO_2 variations but that of sulfates by solubility (Zarga et al. 2013).

Scaling, a frequent development in water is characterised by the looks of the packaging of associate degree adhering crystalline deposit recognized basically by $CaCO_3$ and $CaSO_4{\cdot}2H_2O$ on the surfaces in step with the subsequent reactions.

$$CO_2 + H_2O + CaCO_3 = Ca(HCO_3)_2 \quad (1)$$

$$HCO_3 + H_2O = CO_3 + H_3O^+ \quad (2)$$

$$SO_4 + Ca + 2H_2O = CaSO_4{\cdot}2H_2O \quad (3)$$

All scaling processes by $CaCO_3$ result directly or indirectly from the primary reaction (Eq. (1)). The CO_2 exchange between the liquid and gaseous phases is the main explanation for any scaling. CO_2, in presence of a gasified section, can dissolve within the water. After association and ionization, CO_2 provides rise to associate degree acid product that permits the attack of the current $CaCO_3$ altogether the matter rocks. Then it dissolves and passes within the resolution within the style of carbonate that is way a lot of soluble than the carbonate. This transformation (reaction from left to right in Eq. (1)) corresponds to the matter rocks solubilization method once the water is in contact with atmosphere made in CO_2. If later this water loses the CO_2 by degassing and/or heating, the reaction will move to the other direction (reaction from right to left in combining weight. (1) and offers rise to $CaCO_3$ scale. throughout $CaCO_3$ precipitation, Ca ions can react with carbonate (CO_3^{2-}) ions that accelerate the formation of H_3O^+ ions, as shown in combining weight. (2), resulting in a pH scale decrease throughout germination. Few of the undersaturated carbonate minerals also show definite trends with respect to temperature; atrinite, malachite, hydromagnesite, nesquehonite, $NiCO_3$ and bromides of copper increases with temperature. Natron and witherite show decreasing trend with temperature.

Further, the saturation index of sulfates shows that only barite is saturated; gypsum, anhydrite and celestite show near saturation states (Fig. 3). Other sulfate minerals represented are undersaturated. The variation in temperature shows that there is an increase in saturation sates of the minerals such as anhydrite, celestite, antlerite, chalcanthite,

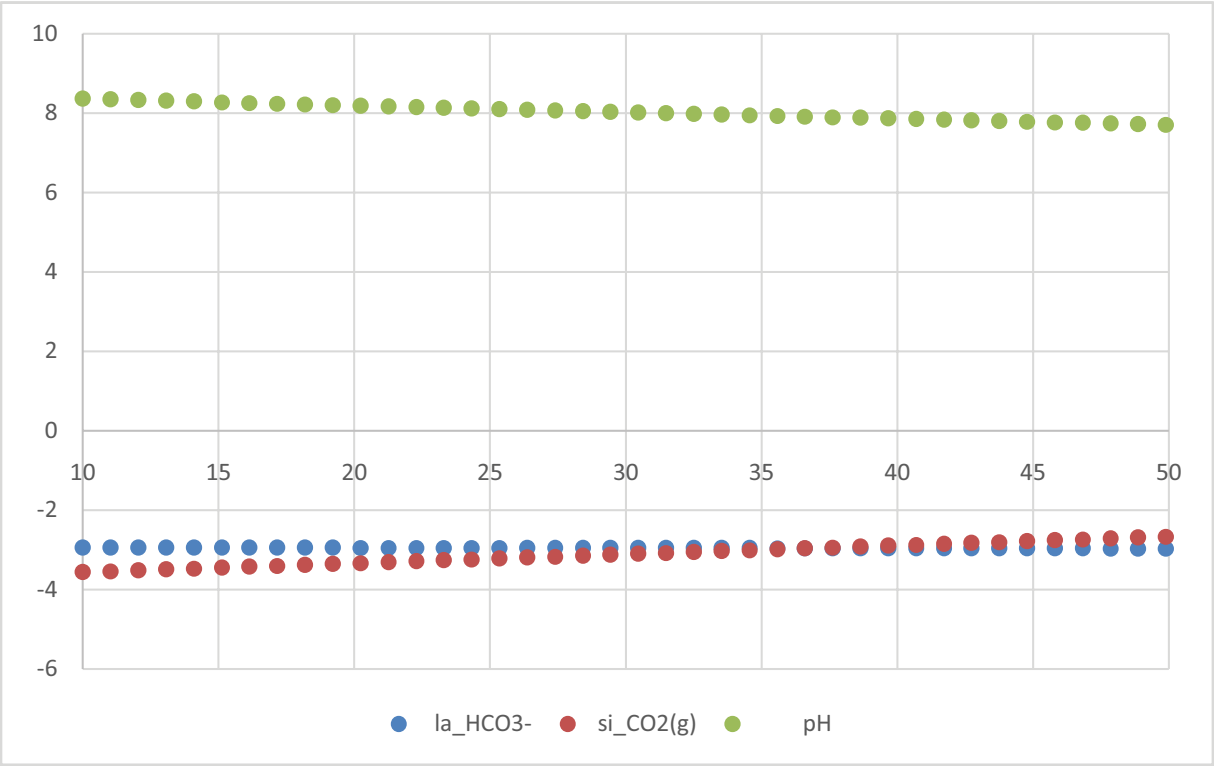

Fig. 2. Variation of pH, HCO_3 and pCO_2 with respect to temperature in °C.

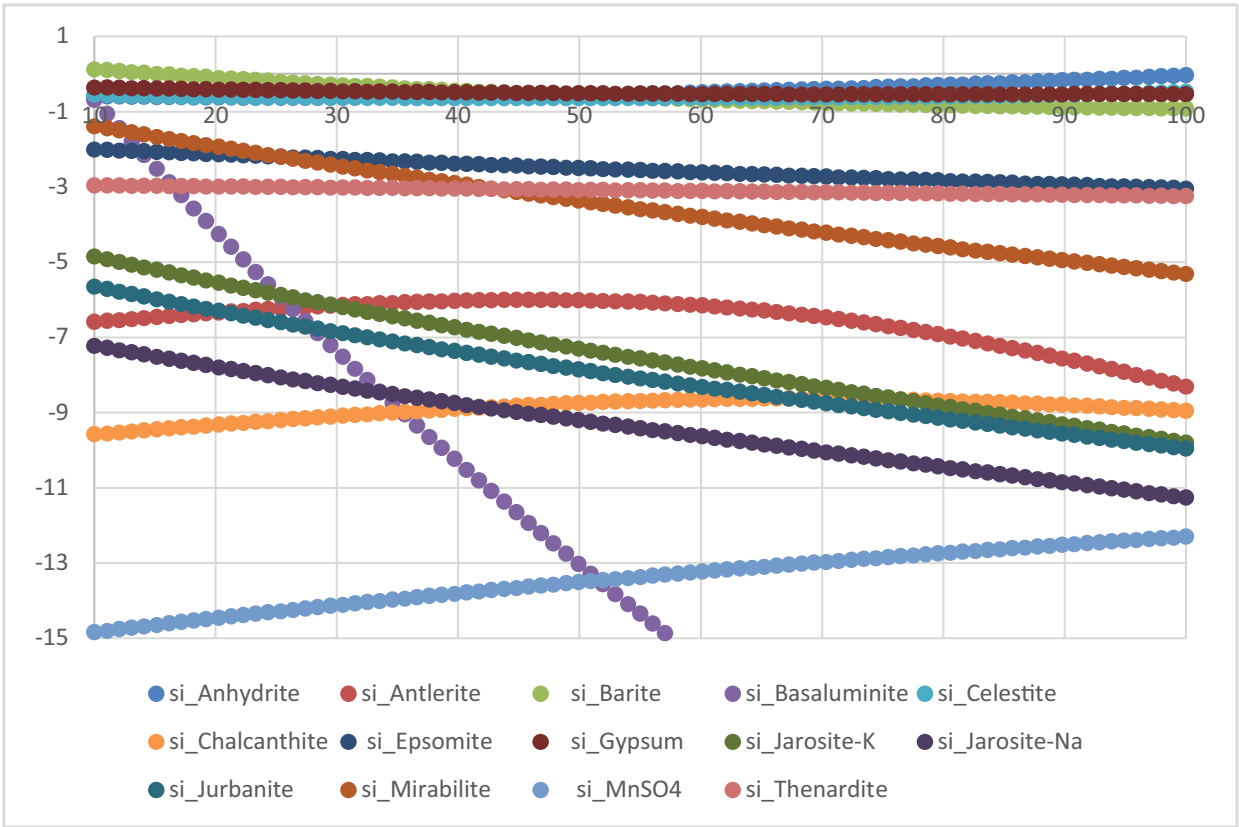

Fig. 3. Variation of the saturation states of sulfate minerals with respect to temperature in °C.

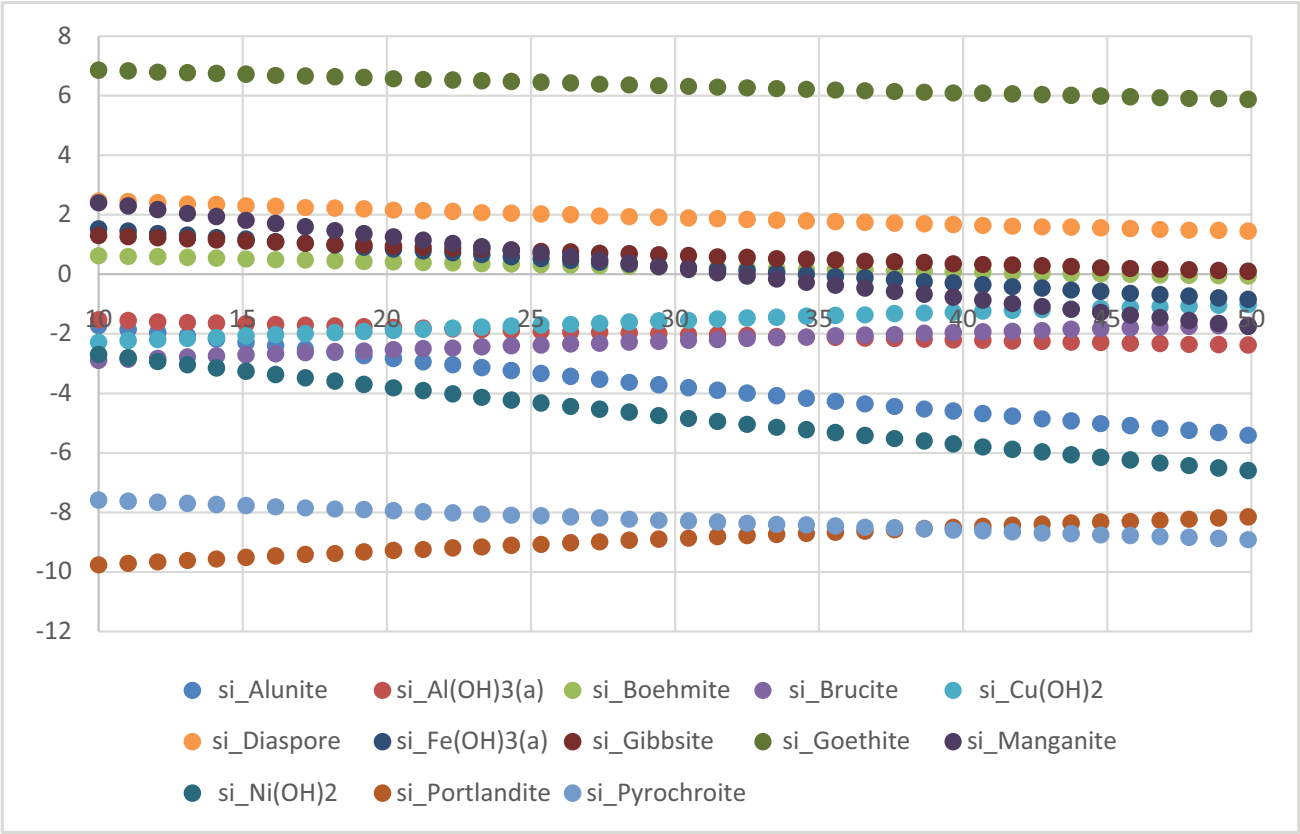

Fig. 4. Variation of the saturation states of hydroxide minerals with respect to temperature in °C.

thenardite and $MnSO_4$ with respect to temperature; whereas other minerals show a decrease, but it is, interesting to note that for this composition considered there is a decrease in saturation index of antlerite beyond 59°C and simultaneously beyond this temperature, there is an increase in saturation index of anhydrite.

Saturation index of hydroxides show that they are saturated with geothite, gibbsite, manganite, boehmite, diaspore, $Fe(OH)_3$ and other hydroxide minerals are undersaturated (Fig. 4). The variation in temperature shows that there is an increase in saturation states of brucite, $Cu(OH)_2$ and portlandite decrease in saturation states with respect to temperature. Oxide mineral saturation states show that they are saturated with composition of hematite, maghemite, magnetite, nsutite, pyrolusite and Bixbyite (Fig. 5). The variation with temperature shows that there is an increase in the saturation sates of the undersaturated minerals such as bunsenite, hausmannite and tenorite. However, all the saturated minerals show decrease in saturation with respect to increase in temperature.

The aluminosilicates show saturations of chlorite, kaolinite, K-mica, leonardite, montmorillonite and phlogopite. The increase in temperature elevates the saturation index of phillipsite, chlorite and pyrophyllite (Fig. 6). The feed water composition also shows saturation of tremolite, talc and chrysolite, which increases with temperature until 30°C and there is a drop in these values. Sepiolite, clinoenstatite and diopside are undersaturated, but the two later minerals increase their saturation beyond 20°C (Fig. 7). The composition of FCO_3 apatite, fluorapatite, hydroxyapatite and fluorite are saturated, but that of SrF_2 are undersaturated (Fig. 8). The temperature relationship to the saturation states of these minerals indicate that there is a decrease in saturation sates of fluorite and FCO_3 apatite.

4. Conclusion

The study on the temperature variation modeling on the average bay water composition shows that the carbonates such as aragonite, calcite, magnesite, huntite, malachite and dolomite; sulfates such as barite and gypsum; hydroxides such as geothite, gibbsite, manganite, boehmite, diaspore and $Fe(OH)_3$; oxides such as hematite, maghemite, magnetite, nsutite, pyrolusite and bixbyite; aluminosilicates such as chlorite, kaolinite, K-mica, leonardite, montmorillonite and phlogopite; silicates such as tremolite, talc and chrysolite along with FCO_3 apatite, fluorapatite, hydroxyapatite and fluorite are inferred to be predominant compositions to be precipitated in the membranes during winter. The increase in saturations are observed in huntite, dolomite, anhydrite, tenorite, pyrophyllite, chlorite, chrysolite and talc are also to be expected during summer as salts in membranes for the solution composition considered. The study reveals the fact that predominantly the dissolution capacities of the feed water have increased during summer resulting in reduced pH and lesser ionic strength under ideal conditions.

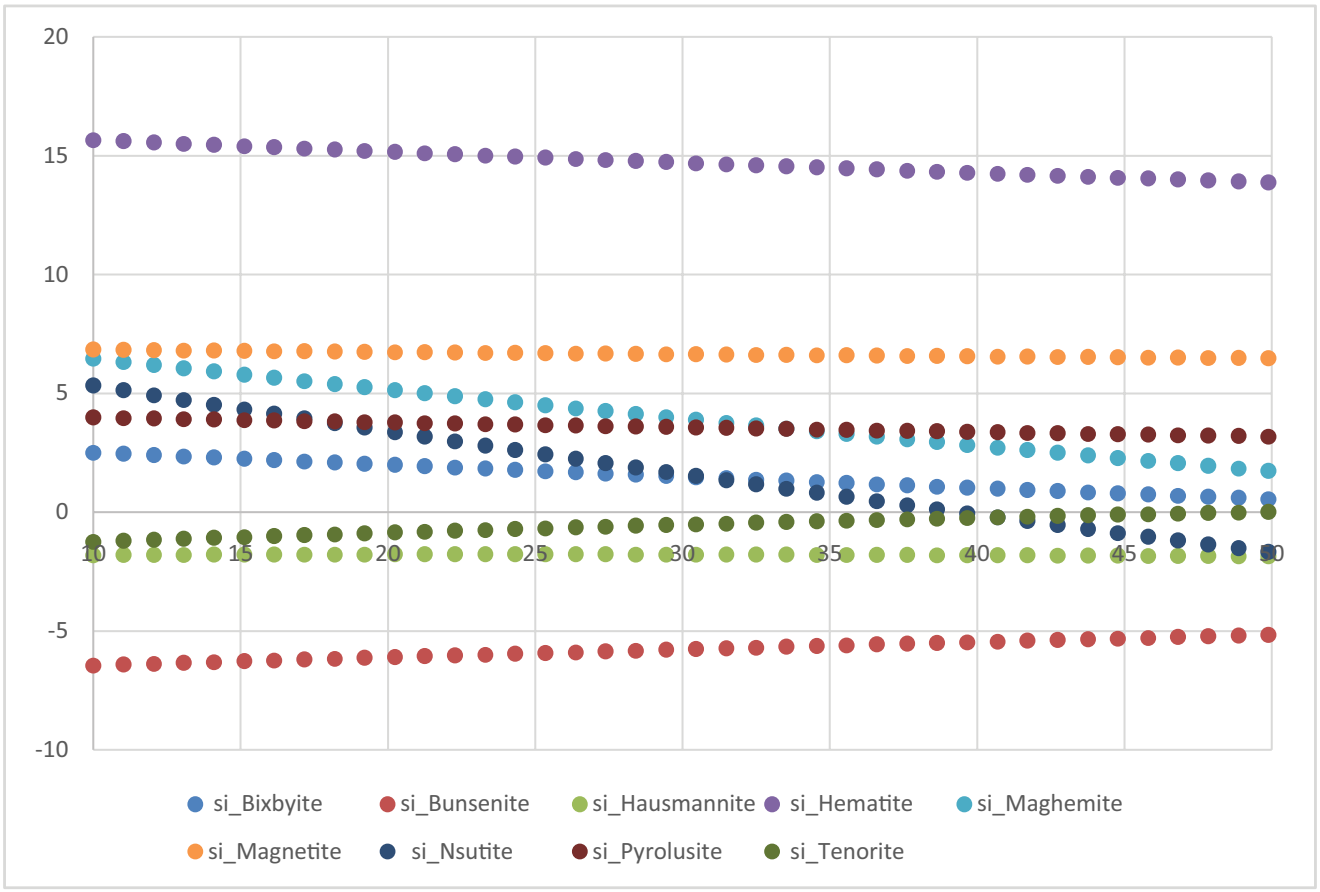

Fig. 5. Variation of the saturation states of oxide minerals with respect to temperature in °C.

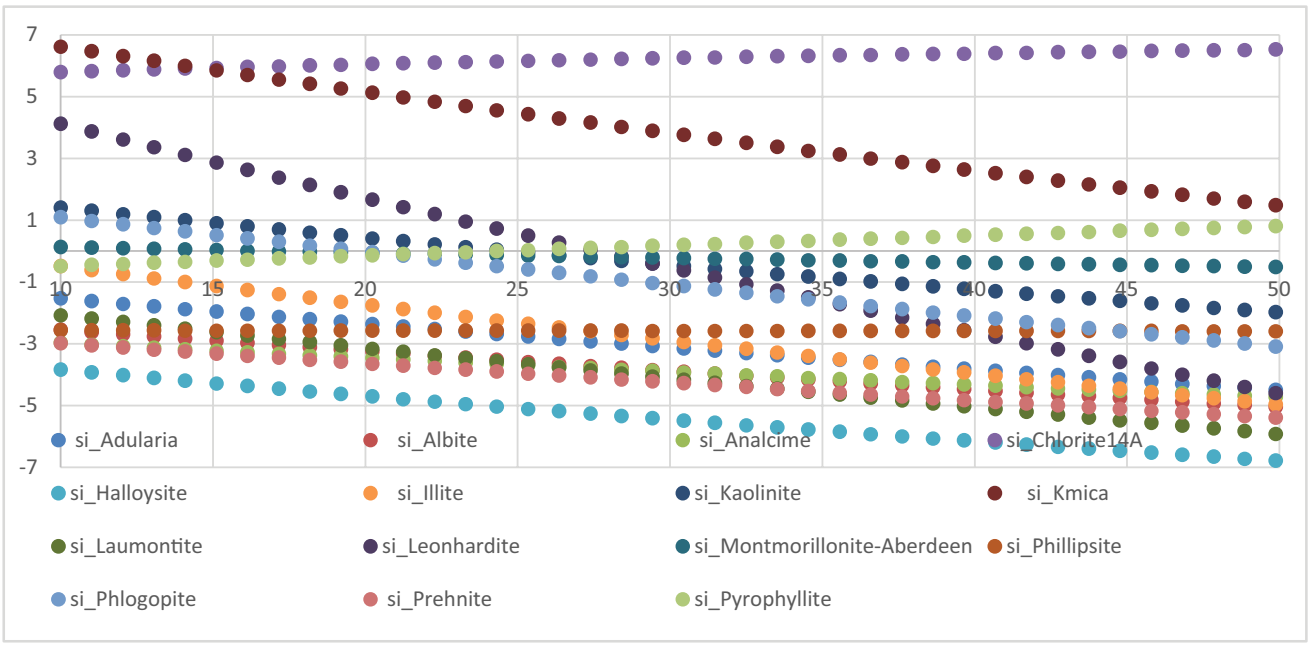

Fig. 6. Variation of the saturation states of aluminosilicate minerals with respect to temperature in °C.

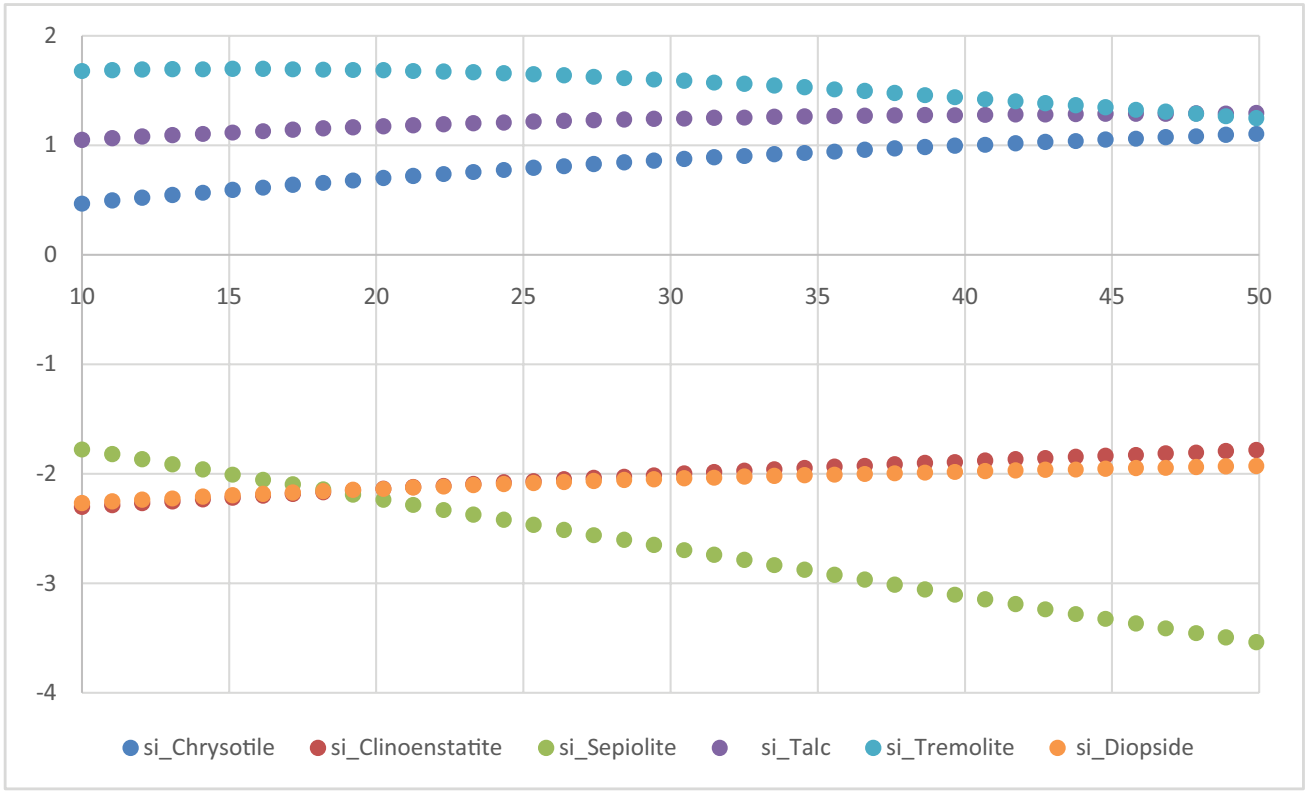

Fig. 7. Variation of the saturation states of silicate mineral minerals with respect to temperature in °C.

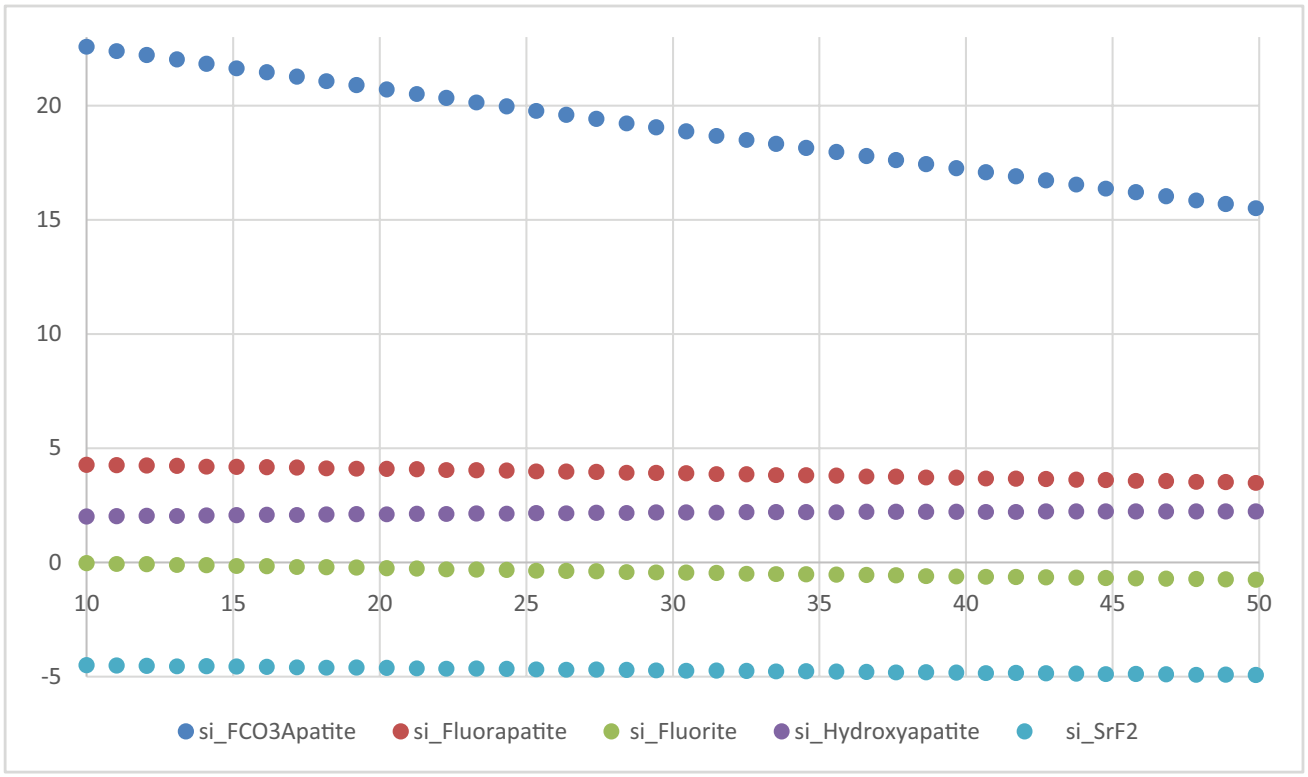

Fig. 8. Variation of the saturation states of fluoride minerals with respect to temperature in °C.

Acknowledgments

The authors would like to express their gratitude to the Kuwait Institute for Scientific Research (KISR), Kuwait, for the financial assistance and to Water Research Center of KISR, for their support in implementation of the study in both lab and field through WM068C. The authors would also like to thank IAEA for their kind support extended for this study through TC project KUW7006.

References

Aiman E. AL-Rawajfeh, Hassan E. S. Fath, and A. A. Mabrouk, 2012, Integrated Salts Precipitation and Nano-Filtration as Pretreatment of Multistage Flash Desalination System. Heat Transfer Engineering, 33(3), 272–279. DOI: 10.1080/01457632.2011.562776.

Alice Antonya, Jor How Lowa, Stephen Gray b, Amy E. Childress C, Pierre Le-Clecha, Greg Lesliea., 2011, Scale formation and control in high pressure membrane water treatment systems: A review. Journal of Membrane Science 383, 1–16.

Amjad Z., Hooley J.,1986, Influence of polyelectrolytes on the crystal growth of calcium sulfate dehydrate. J. Colloid Interface Sci. 111, 496–503.

Astilleros J.M., Fernández-Díaz L., Putnis A., 2010, The role of magnesium in the growth of calcite: an AFM study. Chem. Geol. 271, 52–58.

Chakraborty D., Agarwal V.K., Bhatia S.K., Bellare J.,1994, Steady-state transitions and polymorph transformations in continuous precipitation of calcium carbonate. Ind. Eng. Chem. Res. 33, 2187–2197.

Chen J.C., Li Q., Elimelech M., 2004, In situ monitoring techniques for concentration polarization and fouling phenomena in membrane filtration. Adv. Colloid Interface Sci. 107, 83–108.

Chen T., Neville A., Yuan M., 2006, Influence of Mg^{2+} on $CaCO_3$ formation–bulk precipitation and surface deposition. Chem. Eng. Sci. 61, 5318–5327.

Chidambaram S., Prasanna M.V,. Karmegam U, Singaraja C., Pethaperumal S., Manivannan R., Anandhan P., Tirumalesh K. (2011). "Significance of pCO2 values in determining carbonate chemistry in groundwater of Pondicherry region, India" Frontiers of Earth Science, 5(2), 197–206.

Chong T.H., Wong F.S., Fane A.G., 2007, Enhanced concentration polarization by unstirred fouling layers in reverse osmosis: detection by sodium chloride tracer response technique, J. Membr. Sci. 287, 198–210.

Darton E.G., Fazell M. A, 2001, Statistical review of 150 membrane autopsies. In: 62nd Annual International Water Conference, Pittsburgh.

Dydo P., Turek M., Ciba J., 2003, Scaling analysis of nanofiltration systems fed with saturated calcium sulfate solutions in the presence of carbonate ions. Desalination 159, 245–251.

Greenlee L.F., Lawler D.F., Freeman B.D., Marrot B., Moulin P., 2009, Reverse osmosis desalination: water sources, technology, and today's challenges. Water Res. 43, 2317–2348.

Greenlee L.F., Testa F., Lawler D.F., Freeman B.D., Moulin P., 2010, The effect of antiscalant addition on calcium carbonate precipitation for a simplified synthetic brackish water reverse osmosis concentrate. Water Res. 44, 2957–2969.

Hamdona S.K., Nessim R.B., Hamza S.M., 1993, Spontaneous precipitation of calcium sulphate dihydrate in the presence of some metal ions. Desalination 94, 69–80.

Hoek E.M.V., Allred J., Knoell T., Jeong B.-H., 2008, Modeling the effects of fouling on full-scale reverse osmosis processes. J. Membr. Sci. 314, 33–49.

Klepetsanis P.G., Koutsoukos P.G., 1989, Precipitation of calcium sulfate dihydrate at constant calcium activity. J. Cryst. Growth 98, 480–486.

Klepetsanis, P.G., 1995, The calcite–hydroxypatite system. In: Amjad, Z. (Ed.), Crystal Growth Studies in Aqueous Solution, in Mineral Scale Formation and Inhibition. Plenum Press, New York, pp. 251.

Lee S., C.-H. Lee, 2000, Effect of operating conditions on CaSO4 scale formation mechanism in nanofiltration for water softening. Water Res. 34, 3854–3866.

Lee S., Kim J., Lee C.-H., 1999, Analysis of CaSO4 scale formation mechanism in various nanofiltration modules. J. Membr. Sci. 163, 63–74.

Lee S., Lee C.H., 2005, Scale formation in NF/RO: mechanism and control. Water Sci. Technol. 51, 267–275.

Mucci A., Morse J.W,. 1983, The incorporation of Mg^{2+} and Sr^{2+} into calcite overgrowths: influences of growth rate and solution composition. Geochim. Cosmochim. Acta 47, 217–233.

Nancollas, G.H., Zieba, A., 1995, Constant composition kinetics studies of the simultaneous crystal growth of alkaline earth carbonates and phosphates. In: Amjad, Z. (Ed.), In Mineral Scale Formation. Plenum Press, New York, pp. 1.

Ogino T., Suzuki T., Sawada K., 1987, The formation and transformation mechanism of calcium carbonate in water, Geochim. Cosmochim. Acta 51, 2757–2767.

Oh H.-J., Choung Y.-K., Lee S., Choi J.-S., Hwang T.-M., Kim J.H., 2009, Scale formation in reverse osmosis desalination: model development. Desalination 238, 333–346.

Okazaki M., Kimura S.,1984, Scale formation on reverse-osmosis membranes", J. Chem. Eng. Jpn. 17, 145–151.

Parkhust D.L., Appelo C.A.J., 1999, U.S. Geological Survey, Water Resources Investigations.

Pena J., B. Buil, Garralón A., Gómez P., Turrero M.J., Escribano A., Garralón G., Gómez M.A., 2010, The Vaterite saturation index can be used as a proxy of the S&DSI in sea water desalination by reverse osmosis process. Desalination 254, 75–79.

Pervov A.G., 1991, Scale formation prognosis and cleaning procedure schedules in reverse osmosis systems operation. Desalination 83, 77–118.

Reddy M.M., Nancollas G.H., 1976, The crystallization of calcium carbonate: IV. The effect of magnesium, strontium and sulfate ions. J. Cryst. Growth 35, 33–38.

Rodriguez-Blanco J.D., Shaw S., Benning L.G., 2011, The kinetics and mechanisms of amorphous calcium carbonate (ACC) crystallization to calcite, via Vaterite. Nanoscale 3, 265–271.

Sawada K., 1997, The mechanism of crystallization and transformation of calcium carbonates. Pure Appl. Chem. 69, 921–928.

Sheikholeslami, R., 2003a, Nucleation and kinetics of mixed salts in scaling. AIChE J. 49, 193–194.

Sheikholeslami, R., 2003b, Mixed salts-scaling limits and propensity. Desalination 154, 117.

Sheikholeslami, R., Ng, M., 2001, Calcium sulfate precipitation in the 425 presence of non-dominant calcium carbonate: thermodynamics and kinetics. Ind. Eng. Chem. Res. 40, 3570.

Trusdell, AH. and Jones, BF., 1973, WATEQ: A Computer Program For Calculating Chemical Equlibria Of Natural Waters. J Research US Geological Survey, 2(2), 233 – 248.

Tzotzi C., Pahiadaki T., Yiantsios S.G., Karabelas A.J., Andritsos N., 2007, A study of CaCO3 scale formation and inhibition in RO and NF membrane processes. J. Membr. Sci. 296, 171–184.

Wang X.L., Zhang C., Ouyang P., 2002, The possibility of separating saccharides from a NaCl solution by using nanofiltration in diafiltration mode. J. Membr. Sci. 204, 271–281.

Zarga Y., Ben Boubaker H., Ghaffour N., Elfil H., 2013, Study of calcium carbonate and sulfate co-precipitation. Chemical Engineering Science 96, 33–41.